FLNC-Associated Myofibrillar Myopathy
New Clinical, Functional, and Proteomic Data

Rudolf Andre Kley, MD, Yvonne Leber, PhD, Bertold Schrank, MD, Heidi Zhuge, BSc, Zacharias Orfanos, PhD, Julius Kostan, PhD, Adekunle Onipe, PhD, Dominik Sellung, MD, Anne Katrin Güttsches, MD, Britta Eggers, PhD, Frank Jacobsen, PhD, Wolfram Kress, PhD, Katrin Marcus, PhD, Kristina Djinovic-Carugo, PhD, Peter F.M. van der Ven, PhD, Dieter O. Fürst, PhD, and Matthias Vorgerd, MD

Correspondence
Dr. Kley
rudolf.kley@rub.de

Abstract

Objective
To determine whether a new indel mutation in the dimerization domain of filamin C (FLNc) causes a hereditary myopathy with protein aggregation in muscle fibers, we clinically and molecularly studied a German family with autosomal dominant myofibrillar myopathy (MFM).

Methods
We performed mutational analysis in 3 generations, muscle histopathology, and proteomic studies of IM protein aggregates. Functional consequences of the *FLNC* mutation were investigated with interaction and transfection studies and biophysics molecular analysis.

Results
Eight patients revealed clinical features of slowly progressive proximal weakness associated with a heterozygous c.8025_8030delCAAGACinsA (p.K2676Pfs*3) mutation in *FLNC*. Two patients exhibited a mild cardiomyopathy. MRI of skeletal muscle revealed lipomatous changes typical for MFM with *FLNC* mutations. Muscle biopsies showed characteristic MFM findings with protein aggregation and lesion formation. The proteomic profile of aggregates was specific for MFM-filaminopathy and indicated activation of the ubiquitin-proteasome system (UPS) and autophagic pathways. Functional studies revealed that mutant FLNc is misfolded, unstable, and incapable of forming homodimers and heterodimers with wild-type FLNc.

Conclusions
This new MFM-filaminopathy family confirms that expression of mutant *FLNC* leads to an adult-onset muscle phenotype with intracellular protein accumulation. Mutant FLNc protein is biochemically compromised and leads to dysregulation of protein quality control mechanisms. Proteomic analysis of MFM protein aggregates is a potent method to identify disease-relevant proteins, differentiate MFM subtypes, evaluate the relevance of gene variants, and identify novel MFM candidate genes.

RELATED ARTICLE

Editorial
A Window Into the Myofibrillar Myopathy Proteome
Page e587

From the Department of Neurology (R.A.K., H.Z., D.S., A.K.G., F.J., M.V.), Heimer Institute for Muscle Research, University Hospital Bergmannsheil, Ruhr-University Bochum, Bochum, Germany; Department of Neurology and Clinical Neurophysiology (R.A.K.), St. Marien-Hospital Borken, Borken, Germany; Department of Molecular Cell Biology (Y.L., Z.O., P.F.M.V., D.O.F.), Institute for Cell Biology, University of Bonn, Bonn, Germany; Department of Neurology (B.S.), DKD HELIOS Klinik Wiesbaden, Wiesbaden, Germany; Department of Structural and Computational Biology (J.K., A.O., K.D.-C.), Max Perutz Laboratories, University of Vienna, Vienna, Austria; Medizinisches Proteom-Center (B.E., K.M.), Ruhr-University Bochum, Bochum, Germany; Institute of Human Genetics (W.K.), University of Würzburg, Würzburg, Germany; and Department of Biochemistry (K.D.-C.), Faculty of Chemistry and Chemical Technology, University of Ljubljana, Ljubljana, Slovenia.

Glossary

CK = Creatine kinase; **HGMD** = Human Gene Mutation Database; **MFMs** = Myofibrillar myopathies; **NMD** = nonsense-mediated decay; **NADH** = Nicotinamide adenine dinucleotide dehydrogenase; **SEC-MALS** = size exclusion chromatography combined with multiangle light scatt.

Myofibrillar myopathies (MFMs) are hereditary neuromuscular disorders characterized by intramyoplasmic protein aggregation and focal dissolution of myofibrils.[1-3] A subtype of MFM caused by heterozygous mutations in the *FLNC* gene (MFM5; MIM# 609524) was discovered in 2005,[4] and thereafter, additional families with MFM-filaminopathy were described.[5-9] Main clinical features are progressive skeletal muscle weakness usually manifesting between the fourth and sixth decade of life and respiratory insufficiency in advanced disease stages. MRI reveals a typical pattern of lower limb muscle involvement helpful in differential diagnostics.[6,10-12] Mutations in *FLNC* may also lead to a distal myopathy with histopathologic features distinct from MFM[13,14] or may cause different types of cardiomyopathies.[15]

The *FLNC* gene maps to human chromosome 7q32-q35 and is predominantly expressed in striated muscles. FLNc contains an N-terminal actin-binding domain followed by 24 Ig-like domains that serve as versatile protein interaction interfaces. The carboxyterminal Ig-like domain 24 forms homodimers, enabling filamins to cross-link actin filaments,[16,17] which is a crucial function of the filamins.[11] FLNc binds numerous Z-disc proteins including myopodin/SYNPO2,[18] FATZ/calsarcin/myozenin,[19-21] aciculin/PGM5,[22] and myotilin,[23,24] whereas it interacts at the sarcolemma with components of the dystrophin-dystroglycan complex[25] and acts as scaffold for transmembrane receptors and signaling and adapter proteins.

We characterize the clinical and histopathologic phenotype of a German family with MFM-filaminopathy caused by a novel FLNc mutation in Ig-like domain 24, analyze the molecular pathogenesis, and provide new data about the composition of intramyoplasmic protein aggregates in MFM-filaminopathy.

Patients

A German family with 9 patients representing 3 generations was included in this study (table e-1, links.lww.com/NXG/A410, figure 1A). Six patients underwent neurologic examinations. From patients I:2 and II:3, only medical information from hospital charts was available. Relatives of patient III:3 reported him to be affected, but he refused clinical examination. Five patients had muscle MRI with a 1.5 T MR unit (MAGNETOM Symphony QUANTUM, Siemens) according to previously published protocols.[5]

Figure 1 Pedigree and p.K2676Pfs*3 *FLNC* Mutation Analysis
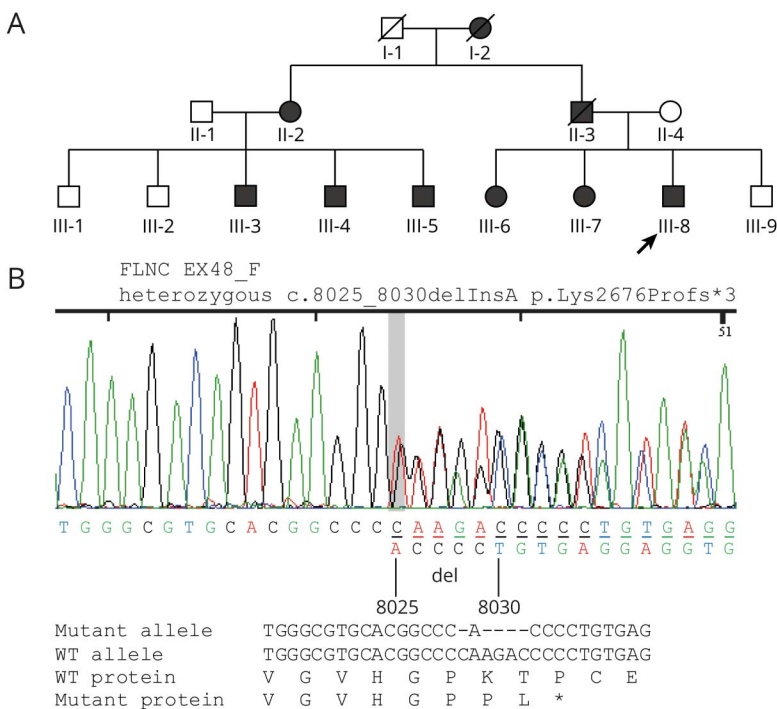
(A) Pedigree of the German family with LGMD-like MFM identified in this study associated with a mutation of *FLNC* exon 48. The index patient III:8 is indicated by an arrow. Individuals with proven mutation and deceased family members who had muscle weakness are represented by filled symbols. (B) Mutation detection via Sanger sequencing with subsequent translation to amino acids in silico.

Methods

Standard Protocol Approvals, Registrations, and Patient Consents

Informed consent was obtained from all patients (approval of Ruhr-University Bochum ethics committee [#4078–11]).

FLNC Mutation Detection

FLNC gene analysis by Sanger sequencing used an established protocol avoiding amplification of the *FLNC* pseudogene.[26] Variant detection was accomplished by aligning the obtained sequence with the NCBI Reference Sequence NM_001458.4 using the software Gensearch (Phenosystems, Braine le Chateau, Belgium).

Muscle Biopsy Studies

Skeletal muscle biopsies from patients III:4 and III:7 were used for evaluating histopathologic changes and for immunolocalization studies, using established procedures.[5,6]

Analysis of Mutant Allele Expression by RT-PCR

Total RNA was purified from muscle samples using the RNeasy fibrous tissue mini kit (Qiagen, Hilden, Germany). Primer pairs used were as follows: (1) ctccagctacagctccatcc and gaggcacttttgggattcaa or (2) catcgtgaacaccctgaatg and gacactttcgtcaccccact. Amplicons were purified, digested with AleI, run on agarose gels, and were analyzed with a gel documentation system (BioRad GelDoc XR) and band densitometry (QuantityOne software).

Cloning of Truncated and Full-Length FLNC Constructs

A *FLNC* d23–24 construct containing the c.8025_8030del-CAAGACinsA mutation was obtained by PCR using primers tttacgcgtGGGGAGCAGAGCCAGGCTGGGGACCCAG (forward) and tttgtcgacCAGGGGTGGGCCGTGCACGCC-CACCATCATC (reverse, without stop codon) or tttgtcgacT-CACAGGGGTGGGCCGTGCACGCCCACCATC (reverse, including stop codon) and the wild-type variant as a template. Amplicons were cloned into the prokaryotic expression vectors pET23-EEF, pET23-T7, or pGEX-6P3 for expression of fusion proteins carrying a C-terminal His-tag and either a C-terminal EEF- or N-terminal T7-immunotag or an N-terminal GST-tag, respectively. Integrity of all constructs was verified by sequencing (LGC Genomics, Berlin, Germany).

Full-length *FLNC* cDNA clones in pEGFP-C2 (Clontech, Takara Holdings, Kyoto, Japan) were obtained as described.[13] The mutation was introduced into full-length *FLNC* by exchanging the cDNA encoding the wild-type Ig-like domains 23–24 with the truncated variant using a unique BspEI restriction site within the cDNA encoding Ig-like domain 23.

Details of expression and purification of recombinant proteins, biophysical characterization, cross-linking of FLNc polypeptides, and proteolytic susceptibility studies are provided in table e-2, links.lww.com/NXG/A411.

Transfection Studies

C2C12 cells were cultured in 6-well plates (TPP, Trasadingen, Switzerland) in Dulbecco's modified Eagle medium supplemented with 15% fetal calf serum, 4 mM L-glutamine, 1% nonessential amino acids, and 2 mM sodium pyruvate (Invitrogen) and transfected with full-length wild-type or mutant *FLNC* constructs (see above) using Lipofectamine LTX and Plus Reagent according to the manufacturer's instructions (Invitrogen). Twenty-four hours after transfection, aggregate formation was evaluated in at least 2,000 transfected cells for each construct by live cell imaging (IX83 microscope, Olympus, Tokyo, Japan). Unpaired *t* tests were used for statistical analysis.

Proteomic Analysis

Differential proteomic analysis was performed with samples of 2 patients carrying the p.K2676Pfs*3 mutation (III:4 and III:7) and 5 patients with distinct *FLNC* mutations (3 with p.W2710X and 2 with p.V930_T933del mutation). The latter patients were also included in our previous proteomic study[27] but were reanalyzed with an optimized method.

Combined laser microdissection label-free mass spectrometry was applied as described.[15,28] 250,000 μm² of protein aggregates and control samples were excised from immunostained 10 μm cryosections by laser microdissection (LMD 6500; Leica Microsystems, Wetzlar, Germany) and transferred to reaction tubes containing 40 μL formic acid (FA, 98%–100%). Samples were incubated at room temperature for 30 minutes in the sonication bath (35 kHz) and centrifuged for 10 minutes (12,000*g*, 4°C), and supernatant proteins were further processed by tryptic digestion[15] or stored at −80°C until use.

Samples were analyzed by nanoHPLC-ESI-MS/MS on an UltiMate 3000 RSLC nanoLC system coupled to a LTQ Orbitrap Elite mass spectrometer (Thermo Fisher Scientific, Bremen, Germany). Protein quantification was performed by spectral counting. Nano LC-MS/MS and subsequent data analysis parameters were as described.[28] Overrepresentation of proteins in aggregate samples was calculated, and a 2-tailed unpaired *t* test (equal variances assumed) was used for each protein. A protein was considered as significantly increased with a fold change >1.5 and *p* value ≤0.05.

Data Availability

Anonymized data not published within this article will be shared by request from any qualified investigator.

Results

Identification of a Novel FLNC Mutation

We describe a 3-generation family with MFM-filaminopathy with 9 affected patients (figure 1A). Sanger sequencing of the *FLNC* gene of the index patient revealed a novel indel mutation c.8025_8030delCAAGACinsA segregating in this family with the disease (figure 1B). This combination of deletion and

Figure 2 Effect of p.K2676Pfs*3 *FLNC* Mutation
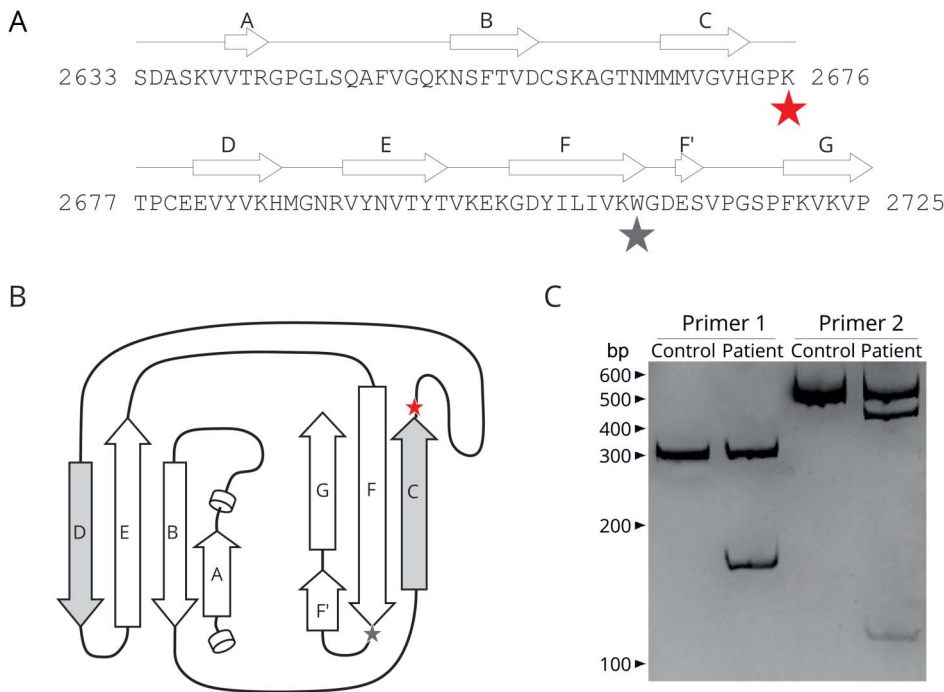
(A and B) Sketch illustrating the effect of the mutation. Topology of filamin C domain 24 as derived from its crystal structure[17] aligned to the amino acid sequence (A) and in a 2-dimensional view (B). β-strands (C and D) form the interface between dimerized domains. Strand G directly interacts with strand (A), which is important for the coherence of the 2 β-sheets that comprise an Ig-like domain. The position of the p.K2676Pfs*3 mutation is marked with a red asterisk. It results in the loss of β-strands (D–G) rendering a correct folding of the domain impossible. The gray asterisk marks the position of the p.W2710X mutation. (C) RT-PCR of control and patient cDNA digested with AleI. cDNA reverse transcribed from control and patient skeletal muscle mRNA amplified with 2 different primer pairs and digested with AleI. Because control cDNA does not contain an AleI restriction site, only mutant cDNA was digested into 160 and 170 bp fragments (primer pair 1) and 450 and 138 bp fragments (primer pair 2), respectively. In patient skeletal muscle, wild-type and mutant mRNA are expressed in an approximate ratio of 4:3.

simultaneous insertion results in a frameshift, producing a premature stop codon at position 2679 (p.K2676Pfs*3).

Similar to the previously reported c.G8130A (p.W2710X) mutation found in several unrelated filaminopathy families, the mutation found in the German family reported here truncates the dimer-forming FLNc Ig-like domain 24. Although in the p.W2710X mutation, the carboxyterminal 16 amino acids are deleted, the c.8025_8030delCAAGACinsA, p.K2676Pfs*3 mutation leads to replacement of the carboxyterminal 50 amino acids by proline and leucine (figure 1B). The mutation therefore results in the deletion of β-strands D, E, F, F′, and G from the Ig-like domain 24 (d24) (figure 2, A and B).

For premature stop codon–causing mutations, it is crucial to check for mutant mRNA degradation via nonsense-mediated decay (NMD). We therefore performed RT-PCR with cDNA from mRNA purified from control and patient skeletal muscles. At the cDNA level, the mutation leads to the generation of an AleI restriction site, enabling us to use different primer pairs to amplify patient and control cDNAs, and a subsequent AleI digestion. Patient cDNA exhibited both wild-type and mutant cDNAs at a ratio of approximately 4:3 (figure 2C), indicating that mutant mRNA is not degraded via NMD and that both wild-type and mutant RNAs are expressed in patients.

Clinical Features

In the 8 affected patients whose data were available, disease onset was diagnosed between 35 to 45 years (mean age 37.4 ± 3.0 years, table e-1, links.lww.com/NXG/A410). In all patients, the initial symptom was proximal leg muscle weakness. The disease course was slowly progressive with additional distal leg and upper limb weakness. At an advanced stage, 3 patients used a wheelchair. Cardiomyopathy occurred in 2/8 patients and respiratory insufficiency in 4/8 patients. Creatine kinase (CK) elevation was moderate and <7-fold of the upper normal limit. Muscle MRI of patient III:4 showed severe symmetrical lipomatous alterations in most posterior thigh muscles (semimembranosus, adductor magnus and longus, semitendinosus, and biceps femoris), in vastus intermedius and in the soleus (figure 3). In lower legs, a reticular pattern of hyperintensity on T1-weighted images was observed in the medial head of gastrocnemius and in tibialis anterior, extensor hallucis longus, and extensor digitorum longus muscles. The pattern of muscle involvement was similar in patient III:5 but ventral thigh muscles, tibialis anterior and the medial head of gastrocnemius were more severely affected than in patient III:4. MRI detected no alterations in the gracilis and in the lateral head of gastrocnemius. In patients with a shorter disease duration, reticular changes occurred either in the anterior tibialis and semimembranosus (III:6) or in the soleus (III:7, III:8) muscle (figure 3) as early degenerative changes.

Histopathologic Studies

Muscle biopsies of patients III:4 and III:7 showed dystrophic-like features with fiber size variation with scattered atrophic and hypertrophic fibers, fiber splitting, increased numbers of centrally located nuclei, augmented fibrosis, and fatty infiltrations. These features were more pronounced in patient III:4 (figure 4A) compared with those in III:7 (figure 4B). Additional structural changes with rimmed vacuoles appeared in some muscle fibers. Trichrome staining (TC) showed muscle

Figure 3 Muscle Imaging Findings in Lower Extremities
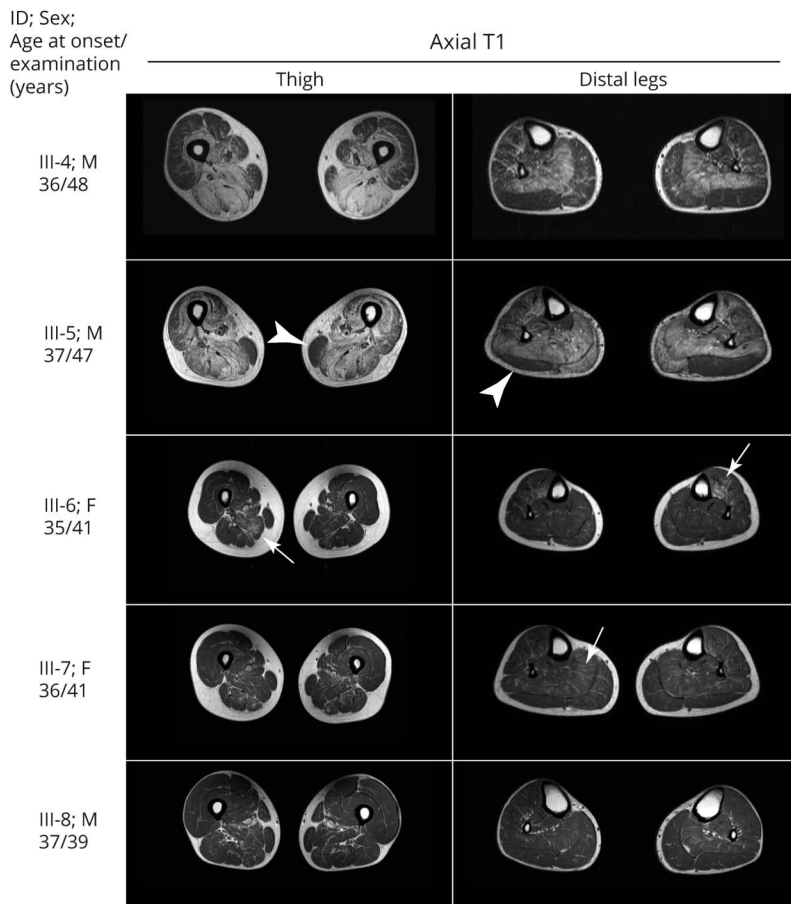
T1-weighted muscle MRI revealed severe fatty degenerative changes in patients III:4 and III:5 with a disease duration of more than 10 years. The gracilis and the lateral head of the gastrocnemius were relatively spared in both patients, as indicated by arrowheads. Mild early changes (arrows) were seen either in the tibialis anterior and semimembranosus (patient III:6) or in the soleus muscle (patients III:7 and III:8).

fibers with a combination of vacuolar changes and blue-colored amorphous deposits (figure 4, A.b and B.b). Nicotinamide adenine dinucleotide dehydrogenase (NADH) staining demonstrated areas devoid of oxidative enzyme activities in many fibers and areas of increased NADH intensities outside these lesions and beneath the sarcolemma (figure 4, A.c and B.c). Immunolocalization studies revealed accumulation of FLNc and desmin in protein aggregates within abnormal muscle fibers (figure 4, C and D.c).

Because muscle fibers of patients with MFM caused by other FLNc mutations and of p.W2711X knock-in mice contain large numbers of myofibrillar lesions, we also stained longitudinal sections of our patients for lesion markers desmin, FLNc (figure 4, E.a-c), myotilin, and Xin (not shown). This revealed that also in patients with p.K2676Pfs*3 mutation, these proteins were not only localized in the typical aggregates but also in frequently occurring microlesions and macrolesions (myofibrillar lesions spanning up to 5 sarcomeres or more than 5 sarcomeres and across multiple myofibrils, respectively).

Proteomic Analysis of Protein Aggregates

Mass spectrometric analysis detected 1045 proteins, with 88 being significantly overrepresented in aggregate samples compared with intraindividual control samples from muscle fibers without aggregates (table e-3, links.lww.com/NXG/A412). From these 88 proteins, the disease-causing FLNc showed the highest mean proportion in aggregates with a value nearly 7-fold higher than in control samples. In relation to proportion, Z-disc and Z-disc–associated proteins represented the most important group of accumulated aggregate proteins, followed by quality control and protein degradation proteins (figure 5). Subgroup analysis of different *FLNC* mutations revealed high similarity of proteomic aggregate profiles in all patients with MFM-filaminopathy (figure 5). Comparison of this MFM-filaminopathy cohort with proteomic findings in 96 other MFM patients, including patients with mutations in other known MFM genes and genetically unresolved cases, revealed that an FLNc ratio (value in aggregate sample divided by the value in intraindividual control sample) above 5 is a highly sensitive (100%) and specific (99%) diagnostic marker for MFM-filaminopathy (data not shown).

Biophysical and Biochemical Studies of Mutant p.K2676Pfs*3 FLNc Protein

We examined effects of the p.K2676Pfs*3 mutation on fold integrity and stability. Circular dichroism spectroscopy was used to assess secondary structure content of the mutant

**Figure 4** Histochemical Findings and Immunolocalization Studies
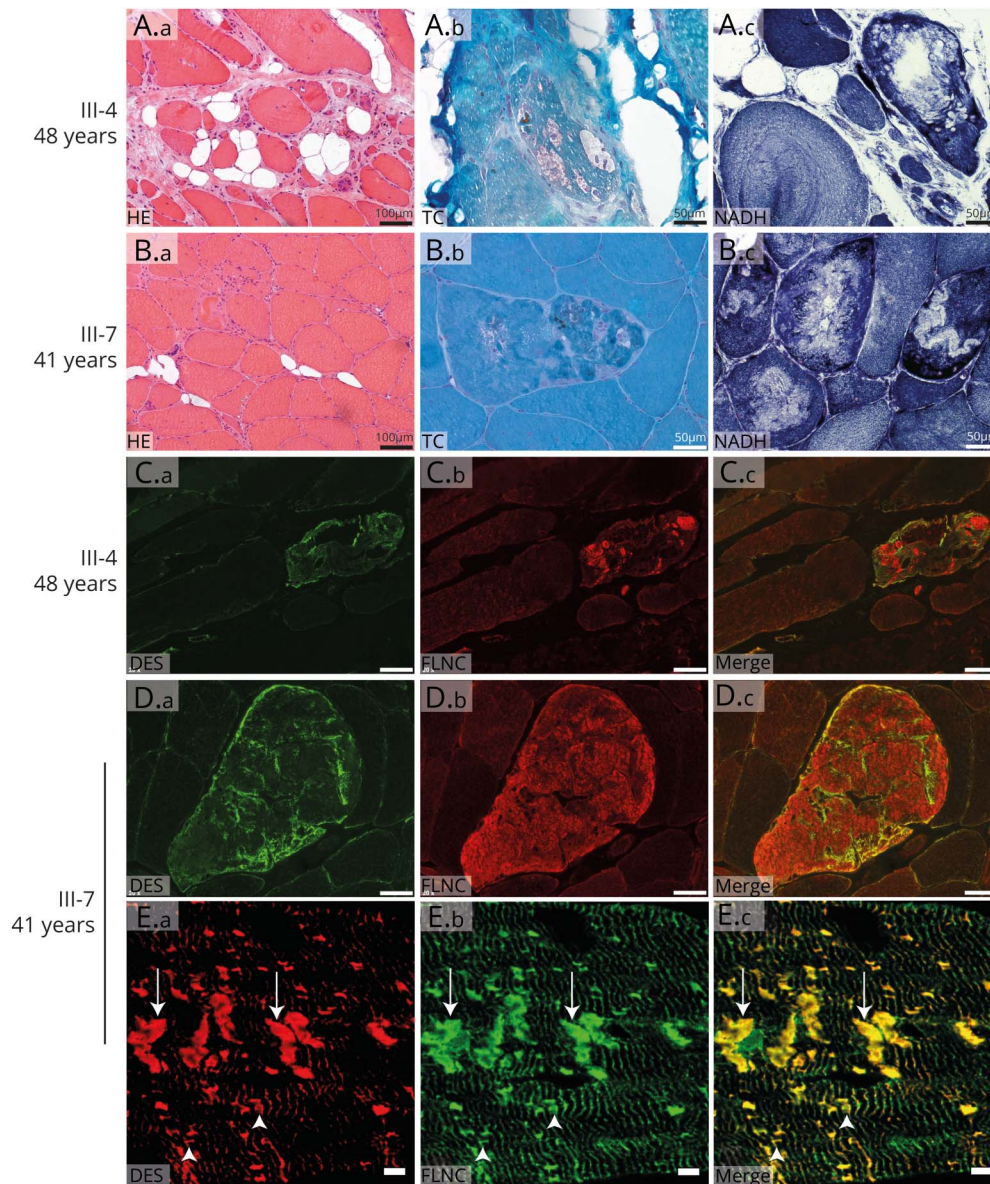
Analysis of muscle biopsy samples from patients III:4 (A and C) and III:7 (B, D, and E). (A.a and B.c) Cryosections stained with H&E, TC, and NADH showed fiber diameter variability, fiber splitting, adipose replacement, endomysial fibrosis, increase in central nuclei, and marked irregularities of the intermyofibrillar network with many fibers showing multiple areas devoid of oxidative enzyme activity. These findings were more pronounced in III:4. (C.a–D.c) Cryosections double stained with antibodies recognizing desmin (DES) and FLNc to localize protein aggregations. Bar: 50 μm. (E.a–E.c) Longitudinal cryosections were double stained for DES and FLNc. Both proteins colocalized in aggregates (arrows), but also in microlesions (arrowheads). Bar: 10 μm.

constructs comprising Ig-like domains 23–24 (d23–24). Whereas analysis of the wild-type domains resulted in the typical ß-strand secondary structure previously reported for these domains,[16,17] the truncated mutant construct resulted in lower signals (figure 6B) for ß-strand structure with a concomitant increase of signal for random coil, suggesting improper folding. Structure stability was analyzed by thermolysin digestion of d23–24 constructs. The mutant p.K2676Pfs*3 protein was already partially digested after 1 minute and completely digested after 20 minutes, whereas a portion of the p.W2710X mutant and almost all of the wild-type variant was still intact after this time (figure 6C),

indicating a notably less stable fold of especially the p.K2676Pfs*3 mutant protein with exposed unfolded regions highly susceptible to proteolysis. We next inspected dimerization of mutant FLNc by chemical cross-linking experiments. Whereas the cross-linking of the wild-type variant yielded a strong signal for dimer and the spontaneous aggregation of the p.W2710X mutant was reproduced, cross-linking of the p.K2676Pfs*3 mutant d23–24 did not yield dimeric cross-links, indicating impaired dimer formation (figure 6D). To assess the hydrodynamic properties and measure the molecular mass of the p.K2676Pfs*3 d23–24 protein in solution, we used size exclusion chromatography

Figure 5 Proteomic Analysis of Skeletal Muscle Samples From Patients With MFM-Filaminopathy
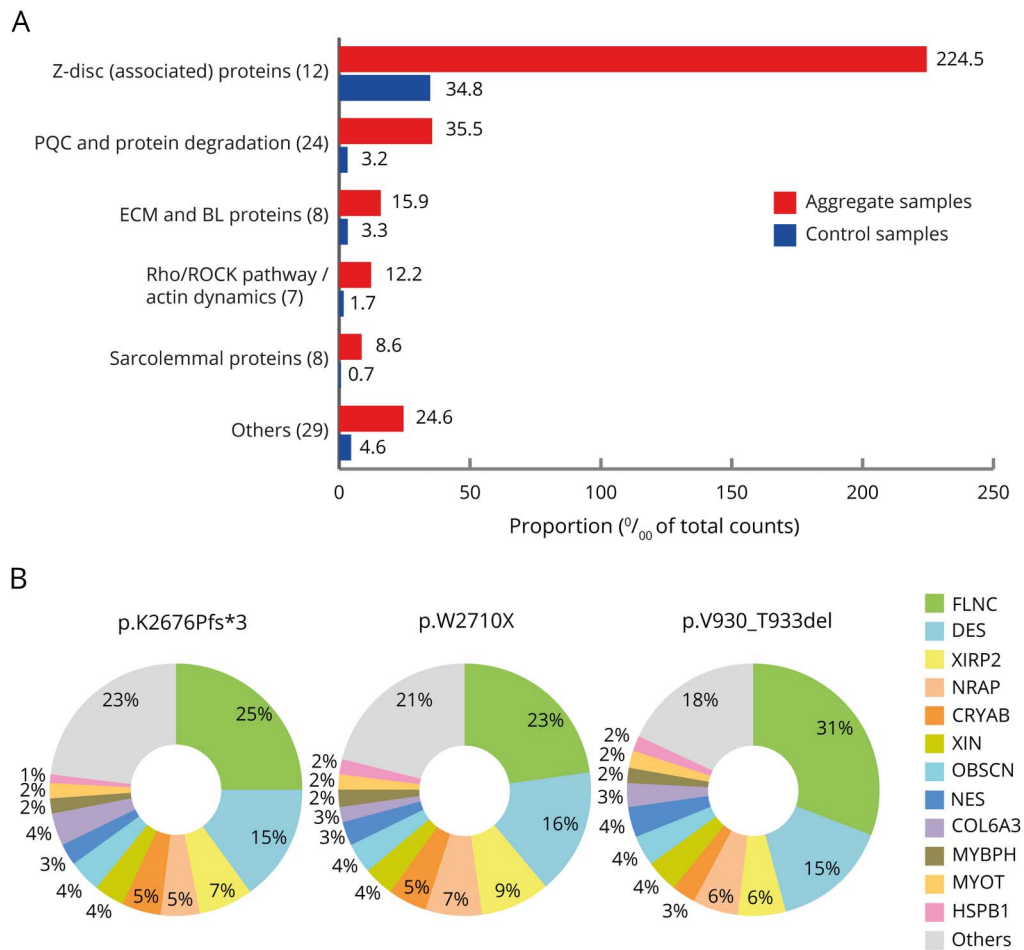
Aggregate and intraindividual control samples were collected by laser microdissection. The bar chart in (A) shows the proportion of proteins identified as overrepresented in aggregate samples (compared with controls), grouped by function. Z-disc and Z-disc–associated proteins were the most abundant components followed by proteins involved in protein quality control and degradation. (B) Proteomic profiles of overrepresented aggregate proteins in patients with filaminopathy caused by different *FLNC* mutations. Pie charts illustrate that the pattern in patients with p.K2676Pfs*3 mutation was highly similar to that in patient with p.W2710X or p.V930_T933del mutation. FLNc was always the most abundant protein, followed by desmin and the FLNc binding partners Xin actin-binding repeat-containing protein 2 (XIRP2) and nebulin-related-anchoring protein (N-RAP). Proportions of αB crystallin, Xin actin-binding repeat-containing protein 1 (Xin), obscurin, and nestin were also similar.

combined with multiangle light scattering (SEC-MALS). Whereas the wild-type construct d23–24 eluted at a volume expected for a dimer and displayed a molecular mass of 48.9 kDa as assessed by MALS, the p.K2676Pfs*3 mutant d23–24 clearly displayed a monomeric state with a nonsymmetric elution profile suggesting a folding defect and structural disorder (figure e-1A, links.lww.com/NXG/A409). Taken together, our data reveal that the deletion mutant is impaired in dimerization due to an incomplete, unfolded domain 24.

Transfection Studies

To analyze effects of expression of mutant FLNc in C2C12 myoblasts, we transiently transfected these cells with constructs encoding full-length wild-type or mutant FLNc. Imaging of more than 5,000 successfully transfected cells revealed that spontaneous aggregate formation was significantly more frequent in cells expressing mutant FLNc

compared with wild-type controls (2.4% vs 1.2%, *p* < 0.0001, figure e-1B, links.lww.com/NXG/A409).

Discussion

Mutations in *FLNC* may lead to MFM, distal myopathy, or a variety of familial and isolated cardiac phenotypes.[7] MFM-filaminopathy is associated with mutations in the rod domain of FLNc causing truncation of the dimerization domain or other protein alterations leading to misfolding and aggregation.[4,8,29] The few reported examples of distal myopathies either result from mutations in the ABD of FLNc,[13] or are caused by haploinsufficiency due to NMD of the mutant transcript.[14] We here describe an MFM-filaminopathy family with a novel indel mutation in one of the exons encoding the dimerization domain of FLNc and characterize its pathogenic consequences.

Figure 6 Functional Studies of the p.K2676Pfs*3 Mutation
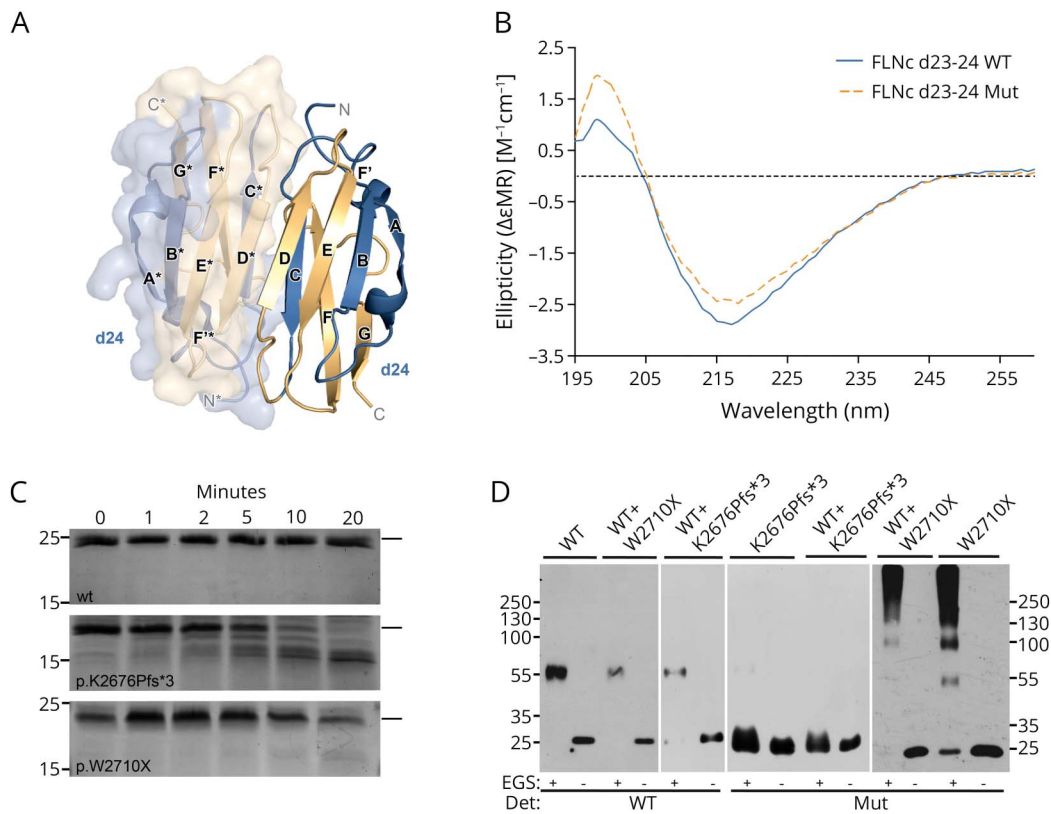
(A) Ribbon representation of the human FLNc domain 24 structure (PDB code 1V05). The d24 dimer is shown in blue with regions missing in the p.K2676Pfs*3 mutant variant shown in light orange. β-strands as well as N and C termini are indicated. Asterisks distinguish β-strands of individual subunits. The mutation leads to loss of β-strands involved in the formation of 2 extended antiparallel β-sheets (B-E-D-D*-E*-B* and C-F-G-G*F*-C*), which stabilize domain fold integrity as well as the dimer, leading to severely impaired dimerization. (B) Circular dichroism spectroscopy performed with purified, bacterially expressed wild-type and p.K2676Pfs*3 mutant FLNc d23–24 constructs. The mean residue ellipticity (ΔεMR) of wild-type and mutant FLNc shows a minimum at 218 nm characteristic of a β-structure. However, the deletion mutant displays a lower amplitude at this wavelength, indicating loss of β-structure and/or folding. (C) Thermolysin digestion of wild-type and mutant FLNc d23–24 for 1–20 minutes. The mutant protein was completely digested after 20 min, whereas almost all the wild-type variant was still intact, and the p.W2710X was only partially digested, indicating less stable folding of the p.K2676Pfs*3 mutant protein. (D) Chemical cross-linking experiments using wild-type (WT) and mutant filamin d23–24 constructs. Without EGS, only monomers of all constructs were detected (approximately 20–25 kDa). After cross-linking with EGS, the wild-type variant appears as dimers (~50 kDa), the mutant p.W2710X construct was mainly found in high-molecular-mass aggregates, and p.K2676Pfs*3 was only found as monomers. In a mixture of differentially tagged wild-type and both mutant constructs (WT + p.W2710X and WT + p.K2676Pfs*3), the wild-type construct dimerizes normally. Note that samples were in part run on different gels that are separated by a white line.

In this family, clinical disease manifestation with proximal lower limb weakness started in the fourth or fifth decade of life. In later disease stages, distal lower limb, upper limb, and respiratory muscles were also involved. A fraction of patients showed cardiac abnormalities, and the CK level was moderately elevated, coinciding with descriptions of MFM-filaminopathy families from different countries and with distinct *FLNC* mutations.[29] This underlines that this type of *FLNC*-associated myopathy, which is associated with the expression of a toxic protein and formation of protein aggregates in muscle fibers, is characterized by a largely homogeneous clinical phenotype differing from the phenotypes caused by mutations in the ABD of *FLNC*,[30] mutations resulting in reduced expression of FLNc protein,[14] or MFM subtypes due to mutations in other genes.[31]

Muscle imaging findings at more advanced disease (III:4 and III:5) were also typical of MFM-filaminopathy with a pattern of muscle involvement that met the criteria defined to differentiate between this disease and other MFM subtypes.[10,12] As in other families with MFM-filaminopathy, the gracilis, sartorius, and the lateral head of the gastrocnemius muscle were relatively spared, although neighboring muscles already showed marked lipomatous changes. Imaging in younger patients with shorter disease duration (III:6, III:7, and III:8) revealed only slight muscle alterations that were not sufficient for a clear distinction against other myopathies, demonstrating the sometimes limited differential diagnostic value of muscle imaging in early disease stages.

The most impressive histopathologic feature in our patients was massive protein aggregation with increased immunoreactivity for FLNc and other MFM marker proteins in their muscle fibers. To further decipher the composition of protein aggregates in MFM-filaminopathy, we extended our previous proteomic studies by analyzing material from these patients and optimizing our approach. From the 88 proteins significantly overrepresented in aggregates, FLNc contributed the highest

quantity of peptides in aggregate samples, followed by further Z-disc and Z-disc–associated proteins. Our previous proteomic studies only identified 28 of these proteins.[27] Several of these newly identified, less abundantly overrepresented proteins are involved in protein degradation and protein quality control, e.g., SQSTM1 (p62), HSPA8 and BAG3. The latter are components of chaperone-assisted selective autophagy (CASA), a tension-induced autophagy pathway essential for myofibril integrity maintenance by degradation of damaged FLNc, and simultaneous stimulation of *FLNC* transcription.[32] These findings are consistent with our previous hypothesis-driven immunolocalization studies in MFM-filaminopathy[29] and with results of proteomic analyses in MFM-myotilinopathy.[28] We succeeded in identifying further chaperones and proteins involved in different cellular pathways as aggregate components. This increases our understanding of the disease pathogenesis and might help to develop new therapeutic strategies, e.g., by influencing CASA activity. Additional interesting proteins overrepresented in aggregate samples are the FLNc binding partners phosphoglucomutase-like protein 5 (PGM5, aciculin) and HSPB7, both being essential for assembly, remodeling and maintenance of myofibrils.[22,33] Furthermore, HSPB7 protein expression levels were highly reduced in muscle fibers of homozygous p.W2711X knock-in mice. Together with the finding that proteins associated with other MFM subtypes (desmin, myotilin, alphaB-crystallin and BAG3) also accumulate in MFM-filaminopathy aggregates, these data render *PGM5* and *HSPB7* promising candidate genes for new MFM subtypes. Therefore, we recommend testing genetically unresolved patients with MFM for mutations in both genes. It is also noteworthy that similar strategies to identify disease genes by combination of laser microdissection and proteomic analysis were already successful in other protein aggregate myopathies (Refs. 34 and 35 and our unpublished data).

Another clinically relevant point is that proteomic analysis can be helpful in differential diagnostic workup of patients with MFM. Our analyses revealed that proteomic aggregate profiles in 7 patients with MFM-filaminopathy with 3 distinct *FLNC* mutations were highly similar. Moreover, we could validate in a large MFM cohort that the FLNc ratio, i.e., the proportion of FLNc in aggregate samples divided by the proportion of FLNc in intraindividual control samples, is a highly sensitive and specific diagnostic biomarker. All patients with MFM-filaminopathy but only 1 of 96 patients with different MFM subtypes had an FLNc ratio above 5. Together with clinical and muscle imaging findings, this biomarker is useful to assess *FLNC* variants of uncertain significance in patients with MFM.

The indel mutation we describe here causes a frameshift introducing a stop codon in the mutant mRNA. In the Human Gene Mutation Database (HGMD; hgmd.cf.ac.uk/ac/index.php), only 1.4% of the total number of human mutations identified are indel mutations, making this type

of mutation very rare.[36] Indeed, in a recent article reporting 325 different variants of the *FLNC* gene, only 4 of those (1.2%) were indel mutations.[7] The region directly flanking the p.K2676Pfs*3 mutation detected in our family (GGTGGGCGTGCACGGCCCC<u>CAAGA</u>CCCCCTGTGA GGAGGTG, deleted nucleotides are underlined) is very GC-rich (72.5%), and stretches of 4 or 5 guanines or cytosines, often flanked by an adenine or thymine, were identified as hotspots for human mutations.[37] It is interesting to note that also 2 different MFM-causing mutations in Ig-like domain 24 of FLNc are localized in a stretch of 4 guanines flanked on both sides by a thymine (NM_001458.4(FLNC):c.8130G>A and c.8129G>A[4,9]). Both mutations result in the same mutation at the protein level (p.W2710X), indicating that this specific stretch of guanines indeed is a mutation hotspot. Because the introduced stop codon occurs in the last exon, NMD does not occur, as confirmed by our RT-PCR experiments, indicating that a misfolded and unstable FLNc variant is indeed expressed, which not only leads to protein aggregation but also results in the formation of numerous myofibrillar lesions. Notably, p.K2676Pfs*3 FLNc was even more susceptible to proteolysis than p.W2710X FLNc. Because muscle fibers of p.W2711X knock-in mice with the latter human FLNc mutation contain myofibrillar lesions, but no aggregates, we proposed that lesions are precursors of aggregates and contribute to muscle weakness.[38] Thus, myofibrillar lesions and protein aggregates are hallmarks of MFM-filaminopathy.

Loss of β-strands F′ and G (figure 2, A and B) caused by the p.W2710X mutation is sufficient for the inability of Ig-like domain 24 to dimerize.[4,39] Instead, multimeric complexes are formed, indicating spontaneous aggregation. Deletion of β-strands D-G in the patients described here also has severe effects: the ability to dimerize is entirely lost, and spontaneous aggregation is displayed in vitro. Indeed, full-length mutant FLNc formed significantly more aggregates in transfected myoblasts than wild-type protein, in line with observed increased levels of proteins involved in degradation and protein quality control in aggregates. Together with our previous data on a mutation in Ig-like domain 7[29,38] and the presence of other MFM-filaminopathy causing mutations in other Ig-like domains,[15] this might indicate that the mere misfolding of any single Ig-like domain of FLNc is sufficient to cause a phenotype with lesion and aggregate formation.

Conclusion

In conclusion, we have identified a rare indel mutation in a potential mutation hotspot in *FLNC* that is associated with MFM-filaminopathy in a German family of 3 subsequent generations. Here, we characterized the disease phenotype and the mutated protein at different levels and found that this mutation causes a pattern typical for various types of protein aggregate-forming MFM-filaminopathies. In addition, we demonstrate a highly similar composition of protein

aggregates in all MFM-filaminopathy subtypes, independent of the individual *FLNC* mutation causative for this disease. Therefore, we suggest this tool as a sensitive and specific diagnostic biomarker in patients with MFM and *FLNC* variants of unknown significance. We also identified promising candidate genes for new MFM subtypes.

Disclosure

R.A. Kley was funded by DFG Research Unit 1228 and received research support from the Heimer foundation. Y. Leber, B. Schrank, H. Zhuge, and Z. Orfanos report no disclosures. J. Kostan was funded by the Welcome Trust Collaborative Award, by Centre of Optimized Structural Studies, and by Austrian-Slovak Interreg Project StruBioMol (B301). A. Onipe was funded by Doctoral Program Plus Structure and Interaction of Biological Macromolecules (W1221). D. Sellung, A.-K. Güttsches, B. Eggers, F. Jacobsen, and W. Kress report no disclosures. K. Marcus was funded by DFG Research Unit 1228. K. Djinovic-Carugo was funded by ITN-MUZIC (N°238423), FWF Projects I525, I1593, P22276, P19060, and W1221, "Laura Bassi Centre of Optimized Structural Studies" (N°253275), Welcome Trust Collaborative Award (201543/Z/16/Z), COST action BM1405, WWTF Chemical Biology project LS17-008, and Christian Doppler Laboratory for High-Content Structural Biology and Biotechnology. P.F.M. van der Ven reports no disclosures. D.O. Fürst was funded by DFG Research Units 1228 and 2743. M. Vorgerd received research support from the Heimer Foundation. Go to Neurology.org/NG for full disclosures.

Appendix Authors

Name	Location	Contribution
Rudolf Andre Kley, MD	Ruhr-University Bochum, Bochum, Germany and St. Marien-Hospital, Borken, Germany	Designed and conceptualized the study; major role in the acquisition and interpretation of data; and drafted the manuscript for intellectual content.
Yvonne Leber, PhD	University of Bonn, Bonn, Germany	Acquisition and interpretation of data and drafted the manuscript for intellectual content.
Bertold Schrank, MD	DKD HELIOS Medical Center Wiesbaden, Wiesbaden, Germany	Acquisition and interpretation of clinical data and drafted the manuscript for intellectual content.
Heidi Zhuge, BSc	Ruhr-University Bochum, Bochum, Germany	Interpretation of data and revised the manuscript for intellectual content.
Zacharias Orfanos, PhD	University of Bonn, Bonn, Germany	Acquisition and interpretation of data.
Julius Kostan, PhD	University of Vienna, Vienna, Austria	Acquisition and interpretation of data.
Adekunle Onipe, PhD	University of Vienna, Vienna, Austria	Acquisition and interpretation of data.
Dominik Sellung, MD	Ruhr-University Bochum, Bochum, Germany	Interpretation of data and revised the manuscript for intellectual content.
Anne Katrin Güttsches, MD	Ruhr-University Bochum, Bochum, Germany	Interpretation of data and revised the manuscript for intellectual content.
Britta Eggers, PhD	Ruhr-University Bochum, Bochum, Germany	Interpretation of proteomic data.
Frank Jacobsen, PhD	Ruhr-University Bochum, Bochum, Germany	Interpretation of data and revised the manuscript for intellectual content.
Wolfram Kress, PhD	University of Würzburg, Würzburg, Germany	Interpretation of data and revised the manuscript for intellectual content.
Katrin Marcus, PhD	Ruhr-University Bochum, Bochum, Germany	Interpretation of proteomic data.
Kristina Djinovic-Carugo, PhD	University of Vienna, Vienna, Austria and University of Ljubljana, Ljubljana, Slovenia	Acquisition and interpretation of data and revised the manuscript for intellectual content.
Peter F.M. van der Ven, PhD	University of Bonn, Bonn, Germany	Acquisition and interpretation of data and revised the manuscript for intellectual content.
Dieter O. Fürst, PhD	University of Bonn, Bonn, Germany	Acquisition and interpretation of data and drafted the manuscript for intellectual content.
Matthias Vorgerd, MD	Ruhr-University Bochum, Bochum, Germany	Major role in the acquisition and analysis of data and drafted the manuscript for intellectual content.

References

1. Kley RA, Olivé M, Schröder R. New aspects of myofibrillar myopathies. *Curr Opin Neurol* 2016;29:628-634.
2. Schröder R, Schoser B. Myofibrillar myopathies: a clinical and myopathological guide. *Brain Pathol* 2009;19:483-492.
3. Selcen D, Engel AG. Myofibrillar myopathies. *Handb Clin Neurol* 2011;101:143-154.
4. Vorgerd M, van der Ven PFM, Bruchertseifer V, et al. A mutation in the dimerization domain of filamin c causes a novel type of autosomal dominant myofibrillar myopathy. *Am J Hum Genet* 2005;77:297-304.
5. Kley RA, Hellenbroich Y, van der Ven PFM, et al. Clinical and morphological phenotype of the filamin myopathy: a study of 31 German patients. *Brain* 2007;130:3250-3264.
6. Kley RA, van der Ven PFM, Olivé M, et al. Impairment of protein degradation in myofibrillar myopathy caused by FLNC/filamin C mutations. *Autophagy* 2013;9:422-423.
7. Verdonschot JAJ, Vanhoutte EK, Claes GRF, et al. A mutation update for the *FLNC* gene in myopathies and cardiomyopathies. *Hum Mutat* 2020;41:1091-1111.
8. Shatunov A, Olivé M, Odgerel Z, et al. In-frame deletion in the seventh immunoglobulin-like repeat of filamin C in a family with myofibrillar myopathy. *Eur J Hum Genet* 2009;17:656-663.
9. Lee HH, Wong S, Sheng B, et al. Clinical and pathological characterization of *FLNC*-related myofibrillar myopathy caused by founder variant c.8129G>A in Hong Kong Chinese. *Clin Genet* 2020;97:747-757.
10. Fischer D, Kley RA, Strach K, et al. Distinct muscle imaging patterns in myofibrillar myopathies. *Neurology* 2008;71:758-765.
11. Fürst DO, Goldfarb LG, Kley RA, Vorgerd M, Olivé M, van der Ven PFM. Filamin C-related myopathies: pathology and mechanisms. *Acta Neuropathol* 2013;125:33-46.
12. Wattjes MP, Kley RA, Fischer D. Neuromuscular imaging in inherited muscle diseases. *Eur Radiol* 2010;20:2447-2460.
13. Duff RM, Tay V, Hackman P, et al. Mutations in the N-terminal actin-binding domain of filamin C cause a distal myopathy. *Am J Hum Genet* 2011;88:729-740.
14. Guergueltcheva V, Peeters K, Baets J, et al. Distal myopathy with upper limb predominance caused by filamin C haploinsufficiency. *Neurology* 2011;77:2105-2114.
15. Maerkens A, Kley RA, Olivé M, et al. Differential proteomic analysis of abnormal intramyoplasmic aggregates in desminopathy. *J Proteomics* 2013;90:14-27.
16. Himmel M, van der Ven PFM, Stocklein W, Fürst DO. The limits of promiscuity: isoform-specific dimerization of filamins. *Biochemistry* 2003;42:430-439.
17. Pudas R, Kiema TR, Butler PJ, Stewart M, Ylanne J. Structural basis for vertebrate filamin dimerization. *Structure* 2005;13:111-119.
18. Linnemann A, van der Ven PFM, Vakeel P, et al. The sarcomeric Z-disc component myopodin is a multiadapter protein that interacts with filamin and alpha-actinin. *Eur J Cell Biol* 2010;89:681-692.
19. Faulkner G, Pallavicini A, Comelli A, et al. FATZ, a filamin-, actinin-, and telethonin-binding protein of the Z-disc of skeletal muscle. *J Biol Chem* 2000;275:41234-41242.
20. Frey N, Olson EN. Calsarcin-3, a novel skeletal muscle-specific member of the calsarcin family, interacts with multiple Z-disc proteins. *J Biol Chem* 2002;277:13998-14004.
21. Takada F, Vander Woude DL, Tong HQ, et al. Myozenin: an alpha-actinin- and gamma-filamin-binding protein of skeletal muscle Z lines. *Proc Natl Acad Sci U S A* 2001;98:1595-1600.
22. Molt S, Bührdel JB, Yakovlev S, et al. Aciculin interacts with filamin C and Xin and is essential for myofibril assembly, remodeling and maintenance. *J Cell Sci* 2014;127:3578-3592.
23. Gontier Y, Taivainen A, Fontao L, et al. The Z-disc proteins myotilin and FATZ-1 interact with each other and are connected to the sarcolemma via muscle-specific filamins. *J Cell Sci* 2005;118:3739-3749.
24. van der Ven PFM, Wiesner S, Salmikangas P, et al. Indications for a novel muscular dystrophy pathway. gamma-filamin, the muscle-specific filamin isoform, interacts with myotilin. *J Cell Biol* 2000;151:235-248.
25. Thompson TG, Chan YM, Hack AA, et al. Filamin 2 (FLN2): a muscle-specific sarcoglycan interacting protein. *J Cell Biol* 2000;148:115-126.
26. Odgerel Z, van der Ven PFM, Fürst DO, Goldfarb LG. DNA sequencing errors in molecular diagnostics of filamin myopathy. *Clin Chem Lab Med* 2010;48:1409-1414.
27. Kley RA, Maerkens A, Leber Y, et al. A combined laser microdissection and mass spectrometry approach reveals new disease relevant proteins accumulating in aggregates of filaminopathy patients. *Mol Cell Proteomics* 2013;12:215-227.
28. Maerkens A, Olivé M, Schreiner A, et al. New insights into the protein aggregation pathology in myotilinopathy by combined proteomic and immunolocalization analyses. *Acta Neuropathol Commun* 2016;4:8.
29. Kley RA, Serdaroglu-Oflazer P, Leber Y, et al. Pathophysiology of protein aggregation and extended phenotyping in filaminopathy. *Brain* 2012;135:2642-2660.
30. van den Bogaart FJ, Claeys KG, Kley RA, et al. Widening the spectrum of filamin-C myopathy: predominantly proximal myopathy due to the p.A193T mutation in the actin-binding domain of *FLNC*. *Neuromuscul Disord* 2017;27:73-77.
31. Walter MC, Reilich P, Huebner A, et al. Scapuloperoneal syndrome type Kaeser and a wide phenotypic spectrum of adult-onset, dominant myopathies are associated with the desmin mutation R350P. *Brain* 2007;130:1485-1496.
32. Ulbricht A, Eppler FJ, Tapia VE, et al. Cellular mechanotransduction relies on tension-induced and chaperone-assisted autophagy. *Curr Biol* 2013;23:430-435.
33. Juo LY, Liao WC, Shih YL, Yang BY, Liu AB, Yan YT. HSPB7 interacts with dimerized FLNC and its absence results in progressive myopathy in skeletal muscles. *J Cell Sci* 2016;129:1661-1670.
34. Greenberg SA, Salajegheh M, Judge DP, et al. Etiology of limb girdle muscular dystrophy 1D/1E determined by laser capture microdissection proteomics. *Ann Neurol* 2012;71:141-145.
35. Schessl J, Zou Y, McGrath MJ, et al. Proteomic identification of FHL1 as the protein mutated in human reducing body myopathy. *J Clin Invest* 2008;118:904-912.
36. Stenson PD, Mort M, Ball EV, et al. The Human Gene Mutation Database: towards a comprehensive repository of inherited mutation data for medical research, genetic diagnosis and next-generation sequencing studies. *Hum Genet* 2017;136:665-677.
37. Ball EV, Stenson PD, Abeysinghe SS, Krawczak M, Cooper DN, Chuzhanova NA. Microdeletions and microinsertions causing human genetic disease: common mechanisms of mutagenesis and the role of local DNA sequence complexity. *Hum Mutat* 2005;26:205-213.
38. Chevessier F, Schuld J, Orfanos Z, et al. Myofibrillar instability exacerbated by acute exercise in filaminopathy. *Hum Mol Genet* 2015;24:7207-7220.
39. Löwe T, Kley RA, van der Ven PFM, et al. The pathomechanism of filaminopathy: altered biochemical properties explain the cellular phenotype of a protein aggregation myopathy. *Hum Mol Genet* 2007;16:1351-1358.